Cell. Mol. Life Sci. 65 (2008) 3961 – 3970
1420-682X/08/243961-10
DOI 10.1007/s00018-008-8593-1

Cellular and Molecular Life Sciences

The role of zinc for alcohol dehydrogenase structure and function

D. S. Auld[a] and T. Bergman[b,*]

[a] Department of Biology, Boston College, Chestnut Hill, Massachusetts 02467 (USA)
[b] Department of Medical Biochemistry and Biophysics, Karolinska Institutet, 171 77 Stockholm (Sweden), Fax: +46 8 337 462, e-mail: Tomas.Bergman@ki.se

Online First 14 November 2008

Abstract. Zinc plays an important role in the structure and function of many enzymes, including alcohol dehydrogenases (ADHs) of the MDR type (medium-chain dehydrogenases/reductases). Active site zinc participates in catalytic events, and structural site zinc maintains structural stability. MDR-types of ADHs have both of these zinc sites but with some variation in ligands and spacing. The catalytic zinc sites involve three residues with different spacings from two separate protein segments, while the structural zinc sites involve four residues and cover a local segment of the protein chain (Cys97-Cys111 in horse liver class I ADH). This review summarizes properties of both ADH zinc sites, and relates them to zinc sites of proteins in general. In addition, it highlights a separate study of zinc binding peptide variants of the horse liver ADH structural zinc site. The results show that zinc coordination of the free peptide differs markedly from that of the enzyme (one His / three Cys versus four Cys), suggesting that the protein zinc site is in an energetically strained conformation relative to that of the peptide. This finding is a characteristic of an entatic state, implying a functional nature for this zinc site.

Keywords. Alcohol dehydrogenase, zinc, metalloenzymes, catalytic zinc site, structural zinc site, entatic state.

Alcohol dehydrogenase of MDR type: a zinc metalloenzyme

Alcohol dehydrogenase (EC 1.1.1.1) of the medium-chain dehydrogenases/reductases (MDR) type catalyzes reversible oxidation of primary and secondary alcohols using the coenzyme NAD(H) [1, 2]. These ADHs are zinc metalloenzymes [3–5] with frequently two tetrahedrally coordinated zinc ions per subunit, one catalytic at the active site, and one structural at a site thought to influence subunit interactions [6, 7]. As in most other zinc metalloenzymes, the catalytic zinc interacts with three protein ligands, one His and two Cys residues, and a water molecule, while the structural zinc interacts with four protein ligands (Tables 1 and 2).

The catalytic zinc binding site for the entire alcohol dehydrogenase family does show some variation. The short spacer varies from 20 to 29 residues, while the long spacer is 84–110 residues (Table 1). The short spacer ligands are Cys and His in all the enzymes. The first ligand (Cys) resides in a loop structure, being the first residue after a β-sheet of 11–13 residues and 2 residues before a 7-residue α-helix. The second ligand (His) is always the first residue before a β-sheet of 10–12 residues (Table 1). The greatest variation in this site comes from the third ligand. In the dehydrogenases using NADP(H), an Asp sometimes replaces the long spacer Cys ligand, and for the polyol dehydrogenase family, the ligand is Glu (Table 1). In the latter family, the Glu may be either the residue adjacent to the His ligand or another Glu, 85 residues away. The crystal structures of the catalytic zinc sites in the ADH family indicate it shifts between two types of coordination where the fourth ligand is either a water molecule or a Glu

* Corresponding author.

Table 1. Catalytic zinc sites of dehydrogenases.[a]

Enzyme	PDB#	L_1	X	L_2	Y	L_3	Z	L_4	Ref.
ADH family									
Class I									
Horse EE	8ADH, 2JHG	Cys_L	20	$His_{b\beta}$	106	Cys_L	–	H_2O	[70, 71]
Cod	1CDO	Cys_L	21	$His_{b\beta}$	106	Cys_L	–	H_2O	[72]
Human									
ADH1A ($\alpha\alpha$)	1HSO, 1UST	Cys_L	20	$His_{b\beta}$	106	Cys_L	–	H_2O	[73, 74]
ADH1B ($\beta_1\beta_1$)	3HUD, 1HSZ	Cys_L	20	$His_{b\beta}$	106	Cys_L	–	H_2O	[73, 75]
ADH1B ($\beta_2\beta_2$)	1HDY	Cys_L	20	$His_{b\beta}$	106	Cys_L	–	H_2O	[76]
ADH1B ($\beta_3\beta_3$)	1HTB	Cys_L	20	$His_{b\beta}$	106	Cys_L	–	H_2O	[77]
ADH1C ($\gamma_2\gamma_2$)	1HT0, 1U3W	Cys_L	20	$His_{b\beta}$	106	Cys_L	–	H_2O	[73, 74]
Class II									
Human	3COS	Cys_L	21	$His_{b\beta}$	110	Cys_L	–	H_2O	*
Mouse	1E3E	Cys_L	20	$His_{b\beta}$	110	Cys_L	–	H_2O	[78]
Class III									
Human ($\chi\chi$)	1TEH	Cys_L	20	$His_{b\beta}$	106	Cys_L	–	Glu_β	[79]
Human glutathione-dependent formaldehyde dehydrogenase	1M6H, 2FZE	Cys_L	21	$His_{b\beta}$	106	Cys_α	–	H_2O	[9, 10]
Pseudomonas putida formaldehyde dehydrogenase	1KOL	Cys_L	20	$His_{b\beta}$	101	Asp_L	–	H_2O	[57]
Class IV									
Human ($\sigma\sigma$)	1AGN	Cys_L	20	$His_{b\beta}$	106	Cys_L	–	H_2O	[80]
Bacterial ADH family									
Bacillus stearothermophilus (LLD-R)	1RJW	Cys_L	22	$His_{b\beta}$	86	Cys_L	–	H_2O	[81]
E. coli protein YAHK	1UUF	Cys_L	21	$His_{b\beta}$	95	Cys_L	–	H_2O	*
Pseudomonas aeruginosa	1LLU	Cys_L	22	$His_{b\beta}$	86	Cys_L	–	H_2O	[82]
Acinetobacter calcoaceticus	1F8F	Cys_L	20	$His_{b\beta}$	106	Cys_L	–	H_2O	*
Thermotoga maritime (TM0436)	1VJ0	Cys_L	21	$His_{b\beta}$	100	Cys_α	–	Glu_β	*
Archaea family									
Sulfolobus solfataricus	1 R37, 1JVB	Cys_L	29	$His_{b\beta}$	85	Cys_L		Glu_β	[83, 84]
Sulfolobus tokodaii (strain 7)	2EER	Cys_L	29	$His_{b\beta}$	85	Cys_L		Glu_β	*
Sulfolobus solfataricus D-arabinose dehydrogenase	2H6E	Cys_L	23	$His_{b\beta}$	84	Cys_L	–	H_2O	[85]
Aeropyrum pernix	1H2B	Cys_L	24	$His_{b\beta}$	88	Asp_L	–	H_2O	[86]
NADP(H)-dependent family									
Amphibian (ADH8)	1P0F	Cys_L	20	$His_{b\beta}$	105	Cys_L	–	H_2O	[87]
Clostridium beijerinckii	1JQB, 1KEV	Cys_L	21	$His_{b\beta}$	90	Asp_L	–	H_2O	[11, 88]
Thermoanaerobacter brockii	1YKF	Cys_L	21	$His_{b\beta}$	90	Asp_L	–	H_2O	[11]
Entamoeba histolytica	1Y9A, 1OUI	Cys_L	21	$His_{b\beta}$	90	Asp_L	–	H_2O	[89, 90]
Saccharomyces cerevisiae Cinnamyl ADH	1Q1N, 1PS0	Cys_L	21	$His_{b\beta}$	94	Cys_L	–	H_2O	[91]
Saccharomyces cerevisiae Yeast ADH I	2HCY	Cys_L	22	$His_{b\beta}$	86	Cys_L	–	H_2O	*
Populus tremuloides Sinapyl ADH	1YQD	Cys_L	21	$His_{b\beta}$	93	Cys_L	–	H_2O	[92]
Arabidopsis thaliana Cinnamyl ADH (AtCAD4 and AtCAD5)	2CF5	Cys_L	21	$His_{b\beta}$	92	Cys_L	–	Glu_β	[93]
Polyol dehydrogenase family									
Bemisia argentifolii or Silverleaf white fly ketose reductase	1E3J	Cys_L	24	$His_{b\beta}$	0	Glu_β	–	H_2O	[94]
Human SDH	1PL8	Cys_L	24	$His_{b\beta}$	0	Glu_β	–	H_2O	[58]
Rat SDH		Cys	24	$His_{b\beta}$	0	Glu_β	–	H_2O	[95]
Sulfolobus solfatarius glucose dehydrogenase	2CD9	Cys_L	26	$His_{b\beta}$	0	Glu_β	–	H_2O	[96]
Thermoplasma acidophilum glucose dehydrogenase		Cys_L	26	$His_{b\beta}$	87	Glu_α	–	H_2O	[16]
Other dehydrogenases									
Bacillus stearothermophilus glycerol dehydrogenase	1JQ5	His_α	17	His_α	82	$Asp_\alpha(N)$	–	H_2O	[97]
Thermotoga maritime glycerol dehydrogenase	1KQ3	His_α	16	His_α	82	$Asp_\alpha(N)$	–	Tris (OH,NH_2)	[98]

[a]PDB# indicates Protein Data Bank accession code. The amino acid spacer between ligands L_1 and L_2 is X; that between L_3 and nearest ligand L_1 or L_2 is Y, and that between L_3 and L_4 is Z. The symbol N indicates that L_3 is located on the amino (N) side of L_2. If no letter is present, L_3 is located on the carboxy-terminal side of L_2. The subscripts α, β refer to the α-3_{10} helix and β-sheet structure which supplies the ligand. The letter subscript L denotes an amino acid sequence of ≤ 8 residues between two structural elements. The subscripts a and b refer to one residue after or before the secondary element. In some ADH structures, the glutamate after the His ligand is observed to bind to the catalytic zinc. This interaction is recorded as Glu being the 4th ligand with no spacer given in order to keep the information on the other 3 ligands consistent with the majority of the structures. *Obtained from PDB structure, paper to be published.

Table 2. Structural zinc sites of dehydrogenases.[a]

Enzyme	PDB#	L_1	X	L_2	Y	L_3	Z	L_4	Ref.
ADH family									
Class I									
Horse EE	8ADH, 2JHG	Cys_L	2	$Cys_{b\alpha}$	2	Cys_α	7	Cys	[70, 71]
Cod	1CDO	Cys_L	2	$Cys_{b\alpha}$	2	Cys_α	7	Cys	[72]
Human									
ADH1A ($\alpha\alpha$)	1HSO, 1UST	Cys_L	2	$Cys_{b\alpha}$	2	Cys_α	7	Cys	[73, 74]
ADH1B ($\beta_1\beta_1$)	3HUD, 1HSZ	Cys_L	2	$Cys_{b\alpha}$	2	Cys_α	7	Cys	[73, 75]
ADH1B ($\beta_2\beta_2$)	1HDY	Cys_L	2	$Cys_{b\alpha}$	2	Cys_α	7	Cys	[76]
ADH1B ($\beta_3\beta_3$)	1HTB	Cys_L	2	$Cys_{b\alpha}$	2	Cys_α	7	Cys	[77]
ADH1C ($\gamma_2\gamma_2$)	1HT0, 1U3W	Cys_L	2	$Cys_{b\alpha}$	2	Cys_α	7	Cys	[73, 74]
Class II									
Human	3COS	Cys_L	2	$Cys_{b\alpha}$	2	Cys_α	7	Cys	*
Mouse	1E3E	Cys_L	2	$Cys_{b\alpha}$	2	Cys_α	7	Cys	[78]
Class III									
Human ($\chi\chi$)	1TEH	Cys_L	2	$Cys_{b\alpha}$	2	Cys_α	7	Cys	[79]
Human glutathione-dependent formaldehyde dehydrogenase	1M6H, 2FZE	Cys_L	2	$Cys_{b\alpha}$	2	Cys_α	7	Cys	[9, 10]
Pseudomonas putida formaldehyde dehydrogenase	1KOL	Cys_L	2	$Cys_{b\alpha}$	2	Cys_α	7	Cys	[57]
Class IV									
Human ($\sigma\sigma$)	1AGN	Cys_L	2	$Cys_{b\alpha}$	2	Cys_α	7	Cys	[80]
Bacterial ADH family									
Bacillus stearothermophilus LLD-R	1RJW	Cys_L	2	$Cys_{b\alpha}$	2	Cys_α	7	Cys	[81]
E. coli protein YAHK	1UUF	Cys_L	2	$Cys_{b\alpha}$	2	Cys_α	7	Cys	*
Pseudomonas aeruginosa	1LLU	Cys_L	2	$Cys_{b\alpha}$	2	Cys_α	7	Cys	[82]
Acinetobacter calcoaceticus	1F8F	Cys_L	2	$Cys_{b\alpha}$	2	Cys_α	7	Cys	*
Thermotoga maritime TM0436	1VJ0	$Cys_{2a\beta}$	2	Cys	2	Cys	8	Cys	*
Thermus thermophilus HB8	2EIH	Cys_L	2	$Cys_{b\alpha}$	2	Cys_α	7	Cys	*
Archaea family									
Sulfolobus solfataricus	1R37,1JVB	Glu_L	2	$Cys_{b\alpha}$	2	Cys_α	7	Cys	[83, 84]
Sulfolobus tokodaii (strain 7)	2EER	Glu_L	2	$Cys_{b\alpha}$	2	Cys_α	7	Cys	*
Sulfolobus solfataricus D-arabinose dehydrogenase	2H6E	Asp_L	2	$Cys_{b\alpha}$	2	Cys_α	7	Cys	[85]
Aeropyrum pernix	1H2B	Asp_L	2	$Cys_{b\alpha}$	2	Cys_α	7	Cys	[86]
NADP(H)-dependent family									
Amphibian (ADH8)	1P0F	Cys_L	2	$Cys_{b\alpha}$	2	Cys_α	7	Cys	[87]
Saccharomyces cerevisiae Cinnamyl ADH	1Q1N, 1PS0	Cys_L	2	$Cys_{b\alpha}$	2	Cys_α	7	Cys	[91]
Saccharomyces cerevisiae Yeast ADH I	2HCY	Cys_L	2	$Cys_{b\alpha}$	2	Cys_α	7	Cys	*
Arabidopsis thaliana Cinnamyl ADH (AtCAD4 and AtCAD5)	2CF5	Cys_L	2	$Cys_{b\alpha}$	2	Cys_α	7	Cys_L	[93]
Populus tremuloides Sinapyl ADH	1YQD	Cys_L	2	$Cys_{b\alpha}$	2	Cys_α	7	Cys_L	[92]
Polyol dehydrogenase family									
Bemisia argentifolii ketose reductase	1E3J	Cys_L	2	$Cys_{b\alpha}$	2	Cys_α	7	Cys_L	[94]
Thermoplasma acidophilum glucose dehydrogenase		Cys	2	Cys	7	Cys	3	$Asp_{b\beta}$	[16]
Sulfolobus solfatarius glucose dehydrogenase	2CD9	Cys_L	2	$Cys_{b\alpha}$	2	Cys_α	7	Cys_L	[96]

[a]See footnote to Table 1 for definitions.

residue (corresponding to Glu68 in horse liver ADH) [8–13]. Moreover, the type of coordination adopted correlates with binding of coenzyme. This in part Glu-coordinated zinc could represent an inactive form of ADH since the zinc ion is displaced about 2 Å from the active site [8], or indicate that Glu coordination during the reaction cycle could have the function of facilitating expulsion of the water and/or the product [12, 13], or of a change to form the coenzyme binding site.

The structural zinc site of ADH was the first such site to be recognized in any protein and led to the definition of structural zinc sites as consisting of one zinc ion bound to four protein ligands but no water [14]. X-ray crystallographic studies reveal that the structural zinc site of horse liver ADH is composed of four closely spaced Cys residues (positions 97, 100, 103, and 111 in a separate loop structure) [7, 15] (Table 2). This site is highly conserved for all classes of the ADH family and for the bacterial enzyme family. The first Cys ligand resides in an 8-amino acid loop, the ligand being positioned 5 residues after a β-sheet of 5 residues, and 4 residues before an α-helix of 4 residues. The second Cys ligand resides immediately before an

α-helix of 4 or 5 residues (Table 2). The third Cys ligand resides in the third position of a 4- or 5-residue α-helix. The last Cys ligand comes from a largely irregular polypeptide segment. The Archaea type of ADHs do show some variation in this site. The first ligand is either an Asp or Glu (Table 2). The fourth ligand is reported to be an Asp for a *Thermoplasma acidophilum* glucose dehydrogenase which also has an altered pattern in the spacing of the ligands (Table 2) [16].

The structural zinc site of ADH has been assigned a role in the maintenance of a proper tertiary/quaternary structure. Early experiments suggested that the zinc ligands are prone to oxidation followed by zinc loss [17], and a similar oxidoreductive interplay between thiols/disulfides was later shown to be a general phenomenon [18] associated with zinc transport in metallothionein [19, 20] and metalloproteins in general [21, 22]. Loss of function through removal of the zinc ion by dialysis was an early argument for its structural importance [5, 6, 23]. Related enzymes not containing this zinc ion, like sorbitol dehydrogenase, display a different quaternary structure [24, 25], and recombinant variants of ADH where one Cys ligand at the time has been changed to Ala, are structurally labile [26].

Since the ligand-altered enzymes are labile, they are not suitable for use in a study of zinc binding to the ADH structural site and its dependence on individual ligands, their spacing, coordination, and associated binding constants. As an alternative, we have examined zinc binding to synthetic peptides corresponding to the structural zinc site of horse liver ADH, with and without amino acid replacements/deletions. The peptide replica of the protein segment (the loop surrounding the structural zinc ion) mimics the metal binding stoichiometry of horse liver ADH [27], and for a peptide set (the 23-residue replica and 17 analogs), zinc stoichiometry, coordination properties and binding affinities were determined and functional interpretations were made [28, 29] (Table 3).

The use of synthetic peptides to study a zinc binding protein segment and its specific metal coordination properties is an approach with several advantages, including experimental flexibility. In the investigation of the horse liver ADH structural zinc site [29], novel insights regarding zinc ligation and potential reactivity in this protein region were obtained, but it was also realized that a careful examination of available three-dimensional structures is vital for interpretations and conclusions. These issues will be discussed in detail after a general background on the multiple roles of zinc in ADHs and metalloproteins in general.

Table 3. Schematic overview of the peptide set studied [29].

Four Cys (peptide replica)	
1. –C-C-C-H-C-	
Three Cys	**One Cys**
2. –A-C-C-H-C	12. –C-A-A-H-A-
3. –C-A-C-H-C	13. –A-C-A-H-A-
4. –C-C-A-H-C-	14. –A-A-C-H-A-
5. –C-C-C-H-A-	15. –A-A-A-H-C-
Two Cys	**Zero Cys**
6. –A-A-C-H-C-	16. –A-A-A-H-A-
7. –C-A-A-H-C-	
8. –C-C-A-H-A-	
9. –A-C-A-H-C	**Zero His**
10. –C-A-C-H-A-	17. –C-C-C-A-C-
11. –A-C-C-H-A	18. –C-C-C-* -C-

*Residues HPE are deleted from the peptide.
The table contains the replica of the zinc binding ADH protein segment FTPQCGKCRVCKHPEGNFCLKND (residues 93–115, Cys ligands underlined) and analogs with replacements/deletions. Only the peptide replica Cys ligands and H105 are shown.

Metalloproteins and zinc

Metals and metalloproteins are receiving increasing recognition for their roles in biological processes. Zinc is after iron the most abundant transition metal in proteins, affecting both structure and function [30, 31]. Since the early experiments with molds by Raulin in 1869 [32], a large amount of data has accumulated showing zinc to be a factor in growth, development and differentiation, and in the transmission of the genetic message in microorganisms, plants and animals [30]. Protein-bound zinc is a key player in a wide range of metabolic processes involving carbohydrates, lipids, proteins and nucleic acids [33], and there are estimates that up to 10% of the human proteome consists of zinc proteins [34, 35].

There are a few distinctive physico-chemical properties of zinc that have a great impact on its reactivity and suitability for catalysis and structural stabilization. The zinc ion (Zn^{2+}) is stable towards reduction and oxidation since it contains a filled *d* orbital (d^{10}), yet it participates in enzymatic redox reactions in combination with organic cofactors [33]. The reactivity of Zn^{2+} is governed by its potential as a Lewis acid (i.e. an electron-pair acceptor), and by its amphoteric properties (i.e. zinc-bound water can exist either as a 'hydronium' ion or a hydroxide ion at physiological pH) [33, 36]. In particular, the fact that the oxidation state of Zn^{2+} does not vary in the highly redox-active environment of a cell is important for its function as a Lewis acid catalyst [37]. Although the cellular redox potential shifts and is in a constant

flux, zinc efficiently fulfills its function as an electrophilic catalyst and stabilizes negative charges that appear during a catalytic cycle [38]. In addition, the filled *d* orbital of zinc results in a ligand-field stabilization energy that is zero in all directions [38]. Hence, the geometry and coordination number of zinc sites can vary greatly since no particular arrangement of the ligands is energetically more favourable than another. This inherent flexibility allows coordination numbers of from 2 to 8 and a multiplicity of accompanying geometries for zinc interactions with small molecules. Our knowledge of zinc structures in proteins suggests that coordination numbers of 4, 5 and 6 are most important to their influence on enzyme structure and function [14, 39–44]. When considering the strength of zinc binding to a protein, its rate of release and its effect on protein structure, one must consider not only the inner shell ligands but also the scaffolding of these sites [43, 45]. The scaffolding encompasses not only the type of secondary structure that supplies the ligands but also the interactions of other amino acids with the inner shell ligands. This fine tuning of zinc ion reactivity and participation in catalytic events involves changes in the charge on the zinc and orientation of the metal ligands [43, 46, 47], and is thus an important determinant for zinc function. Finally, an important factor for the catalytic potential of Zn^{2+} is also the rapid ligand exchange, which allows fast dissociation of products and high turnover numbers [48].

Zinc metalloenzymes are common. Since the discovery of carbonic anhydrase in 1940 by Keilin and Mann [49], about 400 zinc-containing protein structures representing all six enzyme classes and a broad range of phyla and species have been reported [42–44]. The structural data reveal details about the ligands to zinc, zinc binding motifs and the geometry of zinc coordination sites, and in this respect constitute a reference that aids identification of potential zinc binding sites in proteins for which only the amino acid sequences are known [14].

Four distinct types of zinc binding sites in enzymes have thus far been identified: catalytic, cocatalytic, structural and protein interface, and the most frequent amino acid ligands are His, Glu, Asp and Cys [43, 44]. Catalytic zinc sites are generally composed of three protein ligands and a water molecule with His being the predominant ligand. The spacing between the three zinc ligands reveals a pattern composed of a short spacer and a long spacer. The length of the short spacer is often dictated by the type of secondary support structure, 3 for an α-helix and 1 for a β-sheet [36]. In the case of oxidoreductases, the involvement of H-bonding interactions between residues in the short spacer and the presence of the large cofactor, reduced nicotinamide adenine dinucleotide (NADH), may have led to the extension of the short spacer to 16 to 29 residues (Table 1). The short spacer provides a bidentate nucleus for zinc binding, while the long spacer, in addition to making the zinc coordination complete, provides structural flexibility so that protein residues can be aligned for interaction with the substrate or influence the catalytic activity of the zinc ion [50]. The universal water molecule in catalytic zinc sites is activated by ionization, polarization or poised for displacement, and it has been postulated that the activation mechanism is highly dependent on the identity of the other three zinc ligands and their spacing [36, 39]. Structural zinc sites are characterized by four protein ligands and no zinc bound water [14]. While Cys is the most frequent ligand to these sites, in principle a combination of 4 Cys, His, Glu and Asp residues could also form this type of zinc site [51]. Of the 22 permutations of these four ligands, 12 combinations have been observed thus far [51]. The role of the structural zinc site is likely to maintain the structure of the protein in the immediate vicinity, which could in turn effect protein folding. In some cases it may influence enzyme function by supplying enzyme active site residues involved in catalysis which arise from within the spacer arms [51]. Cocatalytic (or coactive) zinc sites are found in enzymes containing two or more zinc and/or other metal atoms (such as manganese) in close proximity to each other and that operate in concert as a catalytic unit [40, 52]. In this type of metal site, the side chain of a single residue, such as Asp, Glu, His or a carboxylated Lys, simultaneously binds (or bridges) both metal ions and thereby determines how far apart the two metals can reside. Sometimes a water molecule forms the bridge between the metal atoms in a cocatalytic site. Asp and His are the most frequent ligands in this type of site [52]. Since the ligands to these sites often come from nearly the whole length of the protein, the metals are important not only to catalytic function but to protein stability. Protein interface is a novel type of zinc binding site that was identified based on the observations that zinc can have an impact on the quaternary structure of a protein [42]. The protein interface zinc binding site thus contains amino acid ligands that reside in the binding surface between two interacting proteins (or protein subunits), and where the ligands are supplied by both proteins (or protein subunits). The coordination properties are generally those of catalytic or structural zinc binding sites [42, 43, 53].

The general importance of zinc in biology, and the fact that zinc in living organisms mainly exists bound to proteins, make characterization of zinc in protein structure and function highly important. Since many zinc-containing proteins are enzymes involved in vital

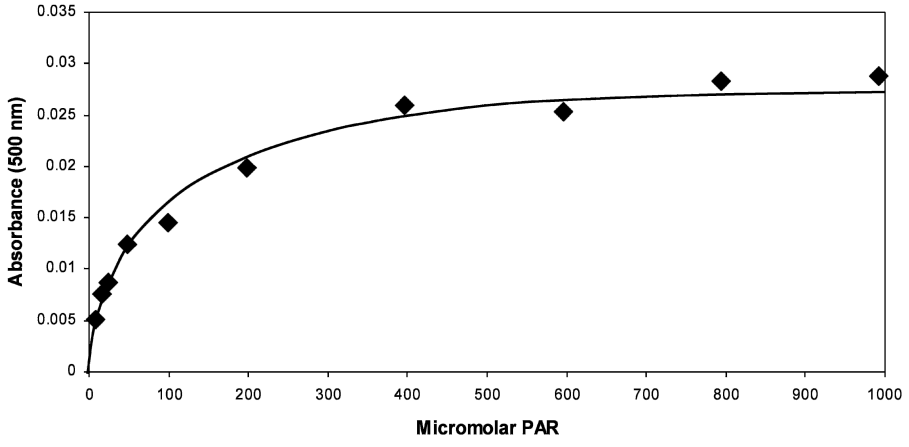

Figure 1. PAR titration of a peptide/zinc complex with four Cys ligands (peptide 17, Tables 3 and 4).

metabolic functions, studies aimed to find rules for zinc ion reactivity and its dependence on the ligands involved, their coordination geometry, and the zinc binding affinity, are important to advance our understanding of catalytic processes and enzyme function, and require specialized methods and strategies.

Zinc binding to alcohol dehydrogenase structural zinc site

The results from examination of zinc binding to synthetic peptides corresponding to the structural zinc site of horse liver ADH, with and without amino acid replacements/deletions, indicate that both the number of Cys residues, the presence of His, and the spacing between Cys/His residues are important variables (Table 3) [29]. The metallochromic chelator 4-(2-pyridylazo)resorcinol (PAR) proves to be effective in direct titration of peptide/zinc complexes and allows the determination of zinc binding constants. Depending on the number and position of ligands, the zinc binding constants range in an ordered fashion from tight to low binding (from 10^{10} to 10^{6} M^{-1}) [29]. Thus, the binding constants determined by competition with PAR reflect the nature of zinc coordination sites.

Exclusion chromatography reveals that all combinations of four, three and two Cys residues generate significant zinc binding [29]. However, X-ray absorption fine structure (XAFS) measurements of the peptide/zinc complexes, using procedures developed for the study of zinc enzymes [54, 55], indicate that the single His residue, corresponding to His105, is a zinc ligand. The presence of His in the peptides results in a three Cys/one His coordination (zinc binding constant (K_B) for the peptide replica is 7.0×10^9 M^{-1}), rather than that of four Cys reported for the protein [15]. When Ala replaces His (peptide 17, Table 4), zinc is still bound (K_B 1.3×10^{10} M^{-1}), and XAFS analysis reveals a distinct four-Cys coordination [29].

The three Cys/one His coordination for the peptide replica leaves one Cys which does not bind. Judging from the zinc stability constants of the three-Cys analogs, Cys103 is a likely candidate (peptide 4, Table 4). When this Cys residue is replaced by Ala, the peptide exhibits almost the same zinc stability as the replica (K_B 6.9×10^9 M^{-1}). Moreover, the XAFS spectra for the peptide replica and the peptide where Ala replaces Cys103 are essentially identical. This further substantiates that replacement of His105 with Ala in peptide 17 (Table 4 and Fig. 1) results in firm zinc binding (of the order 10^{10} M^{-1}) to the four Cys residues as observed in the XAFS analysis.

The coordination of His105 to the zinc in the peptides suggests that its replacement by Cys103 as ligand in the protein is likely to be accompanied by structural strain and higher energy, which could be due to forces exerted upon Cys103 and/or residue 105 in the protein. Analysis of 52 ADH family member sequences using the PIR BLAST and Multiple Alignment programs [56], as well as inspection of three-dimensional

Table 4. Structures, zinc-to-peptide stoichiometries, and zinc binding constants for three of the 18 peptides studied [29].

Peptide	Zinc/ Peptide	K_B Zinc (M^{-1})
Four cysteines (peptide replica)		
1. FTPQ C GK C RV C KHPEGNF C LKND	1.1	7.0×10^9
Three cysteines		
4. FTPQ C GK C RV A KHPEGNF C LKND	1.2	6.9×10^9
Zero histidine		
17. FTPQ C GK C RV C KAPEGNF C LKND	0.9	1.3×10^{10}

The top peptide is the replica of the zinc binding ADH segment (residues 93–115, Cys ligands underlined); the other two contain Cys(103)-to-Ala and His(105)-to-Ala replacements, respectively. Peptide numbers refer to the complete set defined in Table 3.

structures, provides insight into how this zinc coordination might occur and what its function might be [29]. The data reveal that position 105 is not conserved and that Asn (62%), Ser (21%) and His (10%) are the three residues most frequently found at this position. Three-dimensional structures of ADH enzymes exist for the three major variants of residue 105. They show that Cys103 is directed towards the interior of the protein to ligate the zinc, while the side chain of the residue at position 105 is directed to the exterior solvent with its potential zinc binding nitrogen or oxygen of the side chain 11.5–13 Å from the structural zinc ion [29]. Further examination suggests why the residue at position 105 likely exists in this conformation. An α-helix of 14 residues extending from amino acid 324 to 337 places the ε-amino group of Lys323 within H-bonding distance of the amide carbonyl oxygens of residues 103, 105 and 108. While the residues at positions 105 and 108 are not conserved, the interaction of their amide carbonyl oxygen with the ε-amino group of Lys323 is maintained throughout the structures. This interaction directs the side chain of residue 105 to the exterior solvent. Lys323 is conserved in all 52 sequences of the ADH enzymes, further indicating the importance of this interaction. The available three-dimensional structures for class I–IV ADH family members (Table 2) show this same type of interaction with the conserved Lys at the beginning of a 13–14-residue α-helix with the exception of the *Pseudomonas putida* formaldehyde dehydrogenase [57]. In this case Lys323 is replaced by a Phe residue, and only a 6-residue helix is formed. In addition, this helix is now not near the structural zinc site. The aromatic ring of Phe323 is about 28 Å from the amide oxygen of Cys103. In all the bacterial, Archaea, NADP(H) and polyol dehydrogenase families, the Lys residue is generally missing and the helix is either shortened greatly or missing. These are the classes that also have the greatest changes in the structural zinc site. Thus, a Glu or Asp residue substitutes for the first Cys ligand in the Archaea family (Table 2). Human sorbitol dehydrogenase is lacking a structural zinc site since only one Cys residue (position 105) is found in the region of the putative zinc site [58]. No Lys323 is found in this enzyme. Lys329 does reside one amino acid ahead of an α-helix of 9 residues, but the ε-amino group is 48 Å from the amide oxygen of Cys105. The elimination of Lys323 and its associated α-helix maybe related to the changes in the structural zinc site in this type of enzyme.

The PAR titrations and XAFS analysis of the synthetic peptides reveals a strikingly different zinc ligation pattern for the peptides in relation to what is known from the crystal structure of horse liver ADH [15], suggesting that the 'structural' zinc site in the enzyme is in a configuration that is energetically strained relative to that of the peptides. At the present time, we can only speculate as to why this different coordination for the zinc occurs. A post-translational modification of the side chain of residue 105 may occur that is involved in e.g. a binding or a signaling process. Residue 105 in combination with other amino acids on the surface of the protein could also be involved in an as yet unidentified ADH protein complex. In this regard it is of interest to note that for the horse E enzyme, the positively charged side chains of Lys99, Arg101, Lys104 and Lys113 are all directed into the exterior solvent. None of these residues are conserved. Glu99 and Leu101 occur in 65 and 48%, respectively, of the ADH family sequences. Residues 104 and 113 carry a positive charge in 75 and 85%, respectively, of the sequences. All of these residues would be available for interaction with side chains of amino acid residues in another protein.

Modification of the Cys sulfurs by some as yet unidentified means might also occur. This could involve reactions with the bound thiolate ligand or after it is released from the zinc. A prototype for reactions of zinc-bound thiolates is the *Escherichia coli* Ada DNA-repair protein [59]. This protein contains a structural-like zinc site that has the zinc bound to the thiolates of Cys38, Cys42, Cys69 and Cys72 (Protein Data Bank: 1USB). Ada repairs methyl phosphotriester lesions in DNA by transferring the aberrant methyl group to Cys38, which in turn enhances DNA binding by 10^3-fold enabling activation of a methylation resistance regulon [60]. The results of studies on small-molecule methylation reactions have shown that metalation and protonation can differ greatly in their ability to regulate the nucleophilicity of a thiolate [61]. Cys38 can be specifically methylated by CH_3I, while all the other sulfur ligands are unreactive [60]. The presence of an amide N-H in the vicinity (3.1–3.7 Å) of the non-reactive sulfur ligands is believed to be responsible for their inactivity. Examination of a wide variety of zinc finger structures led to the postulate that H-bonds between neighboring amides and thiolate ligands electronically stabilize the thiolates [62, 63]. Further studies of model complexes designed to mimic the binding site of zinc-thiolate proteins show that a single hydrogen bond between an amide N-H and a zinc-coordinated thiolate reduces its reactivity toward an electrophile by up to 2 orders of magnitude [64]. These studies suggest that the zinc thiolates in the ADH structural site should be unreactive towards electrophiles since they have 2–4 amide N-H bonds within 3.1–3.6 Å of each of the zinc-bound thiolates.

In contrast to the deactivating effect of neighboring amide N-H on zinc thiolates, the presence of lysine and arginine side chains within 6.5 Å of Cys residues has been postulated to increase the nucleophilicity of thiolate groups, possibly by enhancing the dissociation of thiol to form the thiolate anion [65]. This type of mechanism would require a Cys ligand to be released from the zinc. The most likely candidate in this case is Cys97, since it is near the exterior solvent and the equivalent residue in a structural zinc site in *E. coli* threonine dehydrogenase has been implicated in forming an air-dependent disulfide bond without loss of enzymatic activity [66]. In addition, the ε-amino group of Lys113 is 4.43 Å from Cys97 in the horse enzyme.

Another driving force for the reaction of the zinc thiolates may be through the proper orientation of an agent capable of reacting with the thiolate. This mechanism would require docking of the agent on the enzyme surface in the proper orientation. Each of the ADH enzyme families has at least two conserved positive charges within 8–12 Å from the thiolate ligands, which could serve as docking residues. The specific modification of the catalytic zinc site thiolate ligand, Cys46, of horse liver ADH by iodoacetic acid likely occurs in this manner [67]. The presence of the neighboring positively charged Arg47 could serve as a docking residue for the carboxylate group of iodoacetic acid, since butandione modification prevents the reaction.

A number of structural zinc sites are indirectly involved in the function of the enzyme through the action of the side chains of the amino acid residues that reside within the spacer arms [43, 51]. Zinc transcription factors also have the properties of a structural zinc site, i.e. four ligands and no bound water molecule. The zinc influences the function of the transcription factor not by direct interaction of the zinc ion with the DNA but rather through the action of residues in its spacer arms to bind to the DNA. Our study [29] shows that the coordination of zinc in the peptide replica of the ADH structural zinc site differs from the coordination seen in the enzyme, suggesting that the structural zinc site in the enzyme is in a strained conformation reminiscent of the entatic state of catalytic zinc sites (i.e. an energized structural condition of an enzyme poised for catalytic action in the absence of substrate) [68, 69]. The results may therefore have implications for an extension of the entatic state hypothesis, originally proposed for active sites, to include also certain structural zinc sites [29].

Acknowledgements. We would like to thank Dr Hans Jörnvall, Karolinska Institutet, for his valuable comments on the manuscript. This work was supported by grants from the Swedish Research Council, the Swedish Cancer Society, NIH grant GM-47534, and the Knut and Alice Wallenberg Foundation.

1 Eklund, H. and Brändén, C.-I. (1979) Structural differences between apo- and holoenzyme of horse liver alcohol dehydrogenase. J. Biol. Chem. 254, 3458–3461.
2 Eklund, H., Samma, J. P., Wallen, L., Brändén, C.-I., Åkeson, Å. and Jones, T. A. (1981) Structure of a triclinic ternary complex of horse liver alcohol dehydrogenase at 2.9 Å resolution. J. Mol. Biol. 146, 561–587.
3 Vallee, B. L. and Hoch, F. L. (1957) Zinc in horse liver alcohol dehydrogenase. J. Biol. Chem. 225, 185–195.
4 Åkeson, Å. (1964) On the zinc content of horse liver alcohol dehydrogenase. Biochem. Biophys. Res. Commun. 17, 211–214.
5 Drum, D. E., Li, T. K. and Vallee, B. L. (1969) Considerations in evaluating the zinc content of horse liver alcohol dehydrogenase preparations. Biochemistry 8, 3783–3791.
6 Sytkowski, A. J. and Vallee, B. L. (1976) Chemical reactivities of catalytic and noncatalytic zinc or cobalt atoms of horse liver alcohol dehydrogenase: differentiation by their thermodynamic and kinetic properties. Proc. Natl. Acad. Sci. USA 73, 344–348.
7 Brändén, C.-I., Jörnvall, H., Eklund, H. and Furugren, B. (1975) Alcohol dehydrogenase. In: The Enzymes, vol. 11, pp. 103–190, Boyer, P. D. (ed.), Academic Press, New York.
8 Karlsson, A., El-Ahmad, M., Johansson, K., Shafqat, J., Jörnvall, H., Eklund, H. and Ramaswamy, S. (2003) Tetrameric NAD-dependent alcohol dehydrogenase. Chem. Biol. Interact. 143–144, 239–245.
9 Sanghani, P. C., Davis, W. I., Zhai, L. and Robinson, H. (2006) Structure-function relationships in human glutathione-dependent formaldehyde dehydrogenase. Role of Glu-67 and Arg-368 in the catalytic mechanism. Biochemistry 45, 4819–4830.
10 Sanghani, P. C., Robinson, H., Bosron, W. F. and Hurley, T. D. (2002) Human glutathione-dependent formaldehyde dehydrogenase. Structures of apo, binary, and inhibitory ternary complexes. Biochemistry 41, 10778–10786.
11 Korkhin, Y., Kalb, A. J., Peretz, M., Bogin, O., Burstein, Y. and Frolow, F. (1998) NADP-dependent bacterial alcohol dehydrogenases: crystal structure, cofactor-binding and cofactor specificity of the ADHs of Clostridium beijerinckii and Thermoanaerobacter brockii. J. Mol. Biol. 278, 967–981.
12 Ryde, U. (1995) On the role of Glu-68 in alcohol dehydrogenase. Protein Sci. 4, 1124–1132.
13 Ryde, U. (1996) The coordination of the catalytic zinc in alcohol dehydrogenase studied by combined quantum-chemical and molecular mechanics calculations. J. Comput. Aided Mol. Des. 10, 153–164.
14 Vallee, B. L. and Auld, D. S. (1990) Zinc coordination, function, and structure of zinc enzymes and other proteins. Biochemistry 29, 5647–5659.
15 Eklund, H., Nordström, B., Zeppezauer, E., Söderlund, G., Ohlsson, I., Boiwe, T., Söderberg, B.-O., Tapia, O., Brändén, C.-I. and Åkeson, Å. (1976) Three-dimensional structure of horse liver alcohol dehydrogenase at 2.4 Å resolution. J. Mol. Biol. 102, 27–59.
16 John, J., Crennell, S. J., Hough, D. W., Danson, M. J. and Taylor, G. L. (1994) The crystal structure of glucose dehydrogenase from Thermoplasma acidophilum [erratum published in Structure (1994) 2, 784]. Structure 2, 385–393.
17 Jörnvall, H. (1973) Differences in thiol groups and multiple forms of rat liver alcohol dehydrogenase. Biochem. Biophys. Res. Commun. 53, 1096–1101.
18 Maret, W. and Vallee, B. L. (1998) Thiolate ligands in metallothionein confer redox activity on zinc clusters. Proc. Natl. Acad. Sci. USA 95, 3478–3482.
19 Jacob, C., Maret, W. and Vallee, B. L. (1998) Control of zinc transfer between thionein, metallothionein, and zinc proteins. Proc. Natl. Acad. Sci. USA 95, 3489–3494.
20 Jiang, L. J., Maret, W. and Vallee, B. L. (1998) The glutathione redox couple modulates zinc transfer from metallothionein to

zinc-depleted sorbitol dehydrogenase. Proc. Natl. Acad. Sci. USA 95, 3483–3488.
21 Jiang, L. J., Vasak, M., Vallee, B. L. and Maret, W. (2000) Zinc transfer potentials of the alpha- and beta-clusters of metallothionein are affected by domain interactions in the whole molecule. Proc. Natl. Acad. Sci. USA 97, 2503–2508.
22 Maret, W. (2004) Zinc and sulfur: a critical biological partnership. Biochemistry 43, 3301–3309.
23 Formicka-Kozlowska, G., Schneider-Bernlöhr, H., von Wartburg, J.-P. and Zeppezauer, M. (1988) $H_8Zn(c)_2$ and $Zn(c)_2$ $Co(n)_2$ human liver alcohol dehydrogenase. Eur. J. Biochem. 173, 281–285.
24 Jeffery, J., Chesters, J., Mills, C., Sadler, P. J. and Jörnvall, H. (1984) Sorbitol dehydrogenase is a zinc enzyme. EMBO J. 3, 357–360.
25 Jörnvall, H., von Bahr-Lindström, H. and Jeffery, J. (1984) Extensive variations and basic features in the alcohol dehydrogenase-sorbitol dehydrogenase family. Eur. J. Biochem. 140, 17–23.
26 Jeloková, J., Karlsson, C., Estonius, M., Jörnvall, H. and Höög, J.-O. (1994) Features of structural zinc in mammalian alcohol dehydrogenase. Site-directed mutagenesis of the zinc ligands. Eur. J. Biochem. 225, 1015–1019.
27 Bergman, T., Jörnvall, H., Holmquist, B. and Vallee, B. L. (1992) A synthetic peptide encompassing the binding site of the second zinc atom (the 'structural' zinc) of alcohol dehydrogenase. Eur. J. Biochem. 205, 467–470.
28 Bergman, T., Palmberg, C., Jörnvall, H., Auld, D. S. and Vallee, B. L. (1999) Zinc binding characteristics of the synthetic peptide corresponding to the structural zinc site of horse liver alcohol dehydrogenase. Adv. Exp. Med. Biol. 463, 339–442.
29 Bergman, T., Zhang, K., Palmberg, C., Jörnvall, H. and Auld, D. S. (2008) Zinc binding to peptide analogs of the structural zinc site in alcohol dehydrogenase: implications for an entatic state. Cell. Mol. Life Sci., this issue.
30 Vallee, B. L. (1988) Zinc: biochemistry, physiology, toxicology and clinical pathology. Biofactors 1, 31–36.
31 Vallee, B. L. and Falchuk, K. H. (1993) The biochemical basis of zinc physiology. Physiol. Rev. 73, 79–118.
32 Raulin, J. (1869) Etudes cliniques sur la vegetation. Ann. Sci. Nat. Bot. Biol. Veg. 11, 93.
33 Vallee, B. L. and Auld, D. S. (1992) Active zinc binding sites of zinc metalloenzymes. Matrix Suppl. 1, 5–19.
34 Andreini, C., Banci, L., Bertini, I. and Rosato, A. (2006) Counting the zinc-proteins encoded in the human genome. J. Proteome Res. 5, 196–201.
35 Andreini, C., Banci, L., Bertini, I. and Rosato, A. (2006) Zinc through the three domains of life. J. Proteome Res. 5, 3173–3178.
36 Vallee, B. L. and Auld, D. S. (1993) Zinc: biological functions and coordination motifs. Acc. Chem. Res. 26, 543–551.
37 Williams, R. J. P. (1987) The biochemistry of zinc. Polyhedron 6, 61–69.
38 Christianson, D. W. (1991) Structural biology of zinc. Adv. Protein Chem. 42, 281–355.
39 Vallee, B. L. and Auld, D. S. (1990) Active-site zinc ligands and activated H_2O of zinc enzymes. Proc. Natl. Acad. Sci. USA 87, 220–224.
40 Vallee, B. L. and Auld, D. S. (1993) New perspective on zinc biochemistry: cocatalytic sites in multi-zinc enzymes. Biochemistry 32, 6493–6500.
41 Auld, D. S. (2001) Zinc sites in metalloenzymes and related proteins. In: Handbook on Metalloproteins, pp. 881–959, Bertini, I., Sigel, A. and Sigel, H. (eds.), Marcel Dekker, New York.
42 Auld, D. S. (2001) Zinc coordination sphere in biochemical zinc sites. BioMetals 14, 271–313.
43 Auld, D. S. (2005) Zinc enzymes. In: Encyclopedia of Inorganic Chemistry, vol. 9, pp. 5885–5927, King, R. B. (ed.), Wiley, Chichester.
44 Patel, K., Kumar, A. and Durani, S. (2007) Analysis of the structural consensus of the zinc coordination centers of metalloprotein structures. Biochim. Biophys. Acta 1774, 1247–1253.
45 Argos, P., Garavito, R. M., Eventoff, W., Rossmann, M. G. and Brändén, C.-I. (1978) Similarities in active center geometries of zinc-containing enzymes, proteases and dehydrogenases. J. Mol. Biol. 126, 141–158.
46 Christianson, D. W. and Fierke, C. A. (1996) Carbonic anhydrase: evolution of the design of the zinc binding site by nature and by design. Acc. Chem. Res. 29, 331–339.
47 McCall, K. A., Huang, C. and Fierke, C. A. (2000) Function and mechanism of zinc metalloenzymes. J. Nutr. 130, 1437S-1446S.
48 Cotton, F. A. and Wilkerson, G. (1988) Advanced Inorganic Chemistry: A Comprehensive Text., vol. 1, Wiley, New York.
49 Keilin, D. and Mann, T. (1940) Carbonic anhydrase. Purification and nature of the enzyme. Biochem. J. 34, 1163–1176.
50 Vallee, B. L. and Auld, D. S. (1989) Short and long spacer sequences and other structural features of zinc binding sites in zinc enzymes. FEBS Lett. 257, 138–140.
51 Auld, D. S. (2004) Structural zinc sites. In: The Handbook of Metalloproteins, vol. 3, pp. 403–415, Messerschmidt, A., Bode, W. and Cygler, M. (eds.), Wiley, Chichester.
52 Auld, D. S. (2004) Cocatalytic zinc sites. In: The Handbook of Metalloproteins, vol. 3, pp. 416–431, Messerschmidt, A., Bode, W. and Cygler, M. (eds.), Wiley, Chichester.
53 Maret, W. (2004) Protein interface zinc sites: the role of zinc in the supramolecular assembly of proteins and in transient protein-protein interactions. In: The Handbook of Metalloproteins, vol. 3, pp. 432–441, Messerschmidt, A., Bode, W. and Cygler, M. (eds.), Wiley, Chichester.
54 Zhang, K. and Auld, D. S. (1993) XAFS studies of carboxypeptidase A: detection of a structural alteration in the zinc coordination sphere coupled to the catalytically important alkaline pKa. Biochemistry 32, 13844–13851.
55 Zhang, K. and Auld, D. S. (1995) Structure of binary and ternary complexes of zinc and cobalt carboxypeptidase A as determined by X-ray absorption fine structure. Biochemistry 34, 16306–16312.
56 The Universal Protein Information Resource: http://pir.georgetown.edu/. Accessed 14 October 2008.
57 Tanaka, N., Kusakabe, Y., Ito, K., Yoshimoto, T. and Nakamura, K. T. (2002) Crystal structure of formaldehyde dehydrogenase from Pseudomonas putida: the structural origin of the tightly bound cofactor in nicotinoprotein dehydrogenases. J. Mol. Biol. 324, 519–533.
58 Pauly, T. A., Ekström, J. L., Beebe, D. A., Chrunyk, B., Cunningham, D., Griffor, M., Kamath, A., Lee, S. E., Madura, R., McGuire, D. et al. (2003) X-ray crystallographic and kinetic studies of human sorbitol dehydrogenase. Structure 11, 1071–1085.
59 Myers, L. C., Terranova, M. P., Ferentz, A. E., Wagner, G. and Verdine, G. L. (1993) Repair of DNA methylphosphotriesters through a metalloactivated cysteine nucleophile. Science 261, 1164–1167.
60 He, C., Hus, J. C., Sun, L. J., Zhou, P., Norman, D. P., Dotsch, V., Wei, H., Gross, J. D., Lane, W. S., Wagner, G. et al. (2005) A methylation-dependent electrostatic switch controls DNA repair and transcriptional activation by E. coli Ada. Mol. Cell. 20, 117–129.
61 Wilker, J. J. and Lippard, S. J. (1997) Alkyl transfer to metal thiolates: kinetics, active species identification, and relevance to the DNA methyl phosphotriester repair center of Escherichia coli Ada. Inorg. Chem. 36, 969–978.
62 Maynard, A. T. and Covell, D. G. (2001) Reactivity of zinc finger cores: analysis of protein packing and electrostatic screening. J. Am. Chem. Soc. 123, 1047–1058.
63 Blake, P. R., Park, J. B., Adams, M. W. W. and Summers, M. F. (1992) Novel observation of NH…S (Cys) hydrogen-bond-mediated scalar coupling in ^{113}Cd-substituted rubredoxin from *Pyrococcus furiosus*. J. Am. Chem. Soc. 114, 4931–4933.
64 Smith, J. N., Hoffman, J. T., Shirin, Z. and Carrano, C. J. (2005) H-bonding interactions and control of thiolate nucleophilicity

and specificity in model complexes of zinc metalloproteins. Inorg. Chem. 44, 2012–2017.
65 Britto, P. J., Knipling, L. and Wolff, J. (2002) The local electrostatic environment determines cysteine reactivity of tubulin. J. Biol. Chem. 277, 29018–29027.
66 Clark-Baldwin, K., Johnson, A. R., Chen, Y.-W., Dekker, E. E. and Penner-Hahn, J. E. (1998) Structural characterization of the zinc site in *Escherichia coli* L-theronine dehydrogenase using extended X-ray absorption fine structure spectroscopy. Inorg. Chim. Acta 275–276, 215–221.
67 Lange, L. G., 3rd, Riordan, J. F., Vallee, B. L. and Brändén, C.-I. (1975) The role of arginyl residues in directing carboxymethylation of horse liver alcohol dehydrogenase. Biochemistry 14, 3497–3502.
68 Vallee, B. L. and Williams, R. J. P. (1968) Metalloenzymes: the entatic nature of their active sites. Proc. Natl. Acad. Sci. USA 59, 498–505.
69 Williams, R. J. P. (1995) Energised (entatic) states of groups and of secondary structures in proteins and metalloproteins. Eur. J. Biochem. 234, 363–381.
70 Colonna-Cesari, F., Perahia, D., Karplus, M., Eklund, H., Brändén, C.-I. and Tapia, O. (1986) Interdomain motion in liver alcohol dehydrogenase. Structural and energetic analysis of the hinge bending mode. J. Biol. Chem. 261, 15273–15280.
71 Meijers, R., Adolph, H. W., Dauter, Z., Wilson, K. S., Lamzin, V. S. and Cedergren-Zeppezauer, E. S. (2007) Structural evidence for a ligand coordination switch in liver alcohol dehydrogenase. Biochemistry 46, 5446–5454.
72 Ramaswamy, S., El-Ahmad, M., Danielsson, O., Jörnvall, H. and Eklund, H. (1996) Crystal structure of cod liver class I alcohol dehydrogenase: substrate pocket and structurally variable segments. Protein Sci. 5, 663–671.
73 Niederhut, M. S., Gibbons, B. J., Perez-Miller, S. and Hurley, T. D. (2001) Three-dimensional structures of the three human class I alcohol dehydrogenases. Protein Sci. 10, 697–706.
74 Gibbons, B. J. and Hurley, T. D. (2004) Structure of three class I human alcohol dehydrogenases complexed with isoenzyme specific formamide inhibitors. Biochemistry 43, 12555–12562.
75 Hurley, T. D., Bosron, W. F., Hamilton, J. A. and Amzel, L. M. (1991) Structure of human beta 1 beta 1 alcohol dehydrogenase: catalytic effects of non-active-site substitutions. Proc. Natl. Acad. Sci. USA 88, 8149–8153.
76 Hurley, T. D., Bosron, W. F., Stone, C. L. and Amzel, L. M. (1994) Structures of three human beta alcohol dehydrogenase variants. Correlations with their functional differences. J. Mol. Biol. 239, 415–429.
77 Davis, G. J., Bosron, W. F., Stone, C. L., Owusu-Dekyi, K. and Hurley, T. D. (1996) X-ray structure of human beta3beta3 alcohol dehydrogenase. The contribution of ionic interactions to coenzyme binding. J. Biol. Chem. 271, 17057–17061.
78 Svensson, S., Höög, J.-O., Schneider, G. and Sandalova, T. (2000) Crystal structures of mouse class II alcohol dehydrogenase reveal determinants of substrate specificity and catalytic efficiency. J. Mol. Biol. 302, 441–453.
79 Yang, Z. N., Bosron, W. F. and Hurley, T. D. (1997) Structure of human chi chi alcohol dehydrogenase: a glutathione-dependent formaldehyde dehydrogenase. J. Mol. Biol. 265, 330–343.
80 Xie, P., Parsons, S. H., Speckhard, D. C., Bosron, W. F. and Hurley, T. D. (1997) X-ray structure of human class IV sigmasigma alcohol dehydrogenase. Structural basis for substrate specificity. J. Biol. Chem. 272, 18558–18563.
81 Ceccarelli, C., Liang, Z. X., Strickler, M., Prehna, G., Goldstein, B. M., Klinman, J. P. and Bahnson, B. J. (2004) Crystal structure and amide H/D exchange of binary complexes of alcohol dehydrogenase from Bacillus stearothermophilus: insight into thermostability and cofactor binding. Biochemistry 43, 5266–5277.
82 Levin, I., Meiri, G., Peretz, M., Burstein, Y. and Frolow, F. (2004) The ternary complex of Pseudomonas aeruginosa alcohol dehydrogenase with NADH and ethylene glycol. Protein Sci. 13, 1547–1556.
83 Esposito, L., Bruno, I., Sica, F., Raia, C. A., Giordano, A., Rossi, M., Mazzarella, L. and Zagari, A. (2003) Crystal structure of a ternary complex of the alcohol dehydrogenase from Sulfolobus solfataricus. Biochemistry 42, 14397–14407.
84 Esposito, L., Sica, F., Raia, C. A., Giordano, A., Rossi, M., Mazzarella, L. and Zagari, A. (2002) Crystal structure of the alcohol dehydrogenase from the hyperthermophilic archaeon Sulfolobus solfataricus at 1.85 Å resolution. J. Mol. Biol. 318, 463–477.
85 Brouns, S. J., Turnbull, A. P., Willemen, H. L., Akerboom, J. and van der Oost, J. (2007) Crystal structure and biochemical properties of the D-arabinose dehydrogenase from Sulfolobus solfataricus. J. Mol. Biol. 371, 1249–1260.
86 Guy, J. E., Isupov, M. N. and Littlechild, J. A. (2003) The structure of an alcohol dehydrogenase from the hyperthermophilic archaeon Aeropyrum pernix. J. Mol. Biol. 331, 1041–1051.
87 Rosell, A., Valencia, E., Pares, X., Fita, I., Farres, J. and Ochoa, W. F. (2003) Crystal structure of the vertebrate NADP(H)-dependent alcohol dehydrogenase (ADH8). J. Mol. Biol. 330, 75–85.
88 Bogin, O., Levin, I., Hacham, Y., Tel-Or, S., Peretz, M., Frolow, F. and Burstein, Y. (2002) Structural basis for the enhanced thermal stability of alcohol dehydrogenase mutants from the mesophilic bacterium Clostridium beijerinckii: contribution of salt bridging. Protein Sci. 11, 2561–2574.
89 Shimon, L. J., Goihberg, E., Peretz, M., Burstein, Y. and Frolow, F. (2006) Structure of alcohol dehydrogenase from Entamoeba histolytica. Acta Crystallogr. D Biol. Crystallogr. 62, 541–547.
90 Goihberg, E., Dym, O., Tel-Or, S., Shimon, L., Frolow, F., Peretz, M. and Burstein, Y. (2008) Thermal stabilization of the protozoan Entamoeba histolytica alcohol dehydrogenase by a single proline substitution. Proteins 72, 711–719.
91 Valencia, E., Larroy, C., Ochoa, W. F., Pares, X., Fita, I. and Biosca, J. A. (2004) Apo and Holo structures of an NADPH-dependent cinnamyl alcohol dehydrogenase from Saccharomyces cerevisiae. J. Mol. Biol. 341, 1049–1062.
92 Bomati, E. K. and Noel, J. P. (2005) Structural and kinetic basis for substrate selectivity in Populus tremuloides sinapyl alcohol dehydrogenase. Plant Cell 17, 1598–1611.
93 Youn, B., Camacho, R., Moinuddin, S. G., Lee, C., Davin, L. B., Lewis, N. G. and Kang, C. (2006) Crystal structures and catalytic mechanism of the Arabidopsis cinnamyl alcohol dehydrogenases AtCAD5 and AtCAD4. Org. Biomol. Chem. 4, 1687–1697.
94 Banfield, M. J., Salvucci, M. E., Baker, E. N. and Smith, C. A. (2001) Crystal structure of the NADP(H)-dependent ketose reductase from Bemisia argentifolii at 2.3 Å resolution. J. Mol. Biol. 306, 239–250.
95 Johansson, K., El-Ahmad, M., Kaiser, C., Jörnvall, H., Eklund, H., Höög, J.-O. and Ramaswamy, S. (2001) Crystal structure of sorbitol dehydrogenase. Chem. Biol. Interact. 130–132, 351–358.
96 Milburn, C. C., Lamble, H. J., Theodossis, A., Bull, S. D., Hough, D. W., Danson, M. J. and Taylor, G. L. (2006) The structural basis of substrate promiscuity in glucose dehydrogenase from the hyperthermophilic archaeon Sulfolobus solfataricus. J. Biol. Chem. 281, 14796–14804.
97 Ruzheinikov, S. N., Burke, J., Sedelnikova, S., Baker, P. J., Taylor, R., Bullough, P. A., Muir, N. M., Gore, M. G. and Rice, D. W. (2001) Glycerol dehydrogenase: structure, specificity, and mechanism of a family III polyol dehydrogenase. Structure 9, 789–802.
98 Lesley, S. A., Kuhn, P., Godzik, A., Deacon, A. M., Mathews, I., Kreusch, A., Spraggon, G., Klock, H. E., McMullan, D., Shin, T. et al. (2002) Structural genomics of the Thermotoga maritima proteome implemented in a high-throughput structure determination pipeline. Proc. Natl. Acad. Sci. USA 99, 11664–11669.